International Journal of Thermal Technologies
E-ISSN 2277 – 4114

Available at http://inpressco.com/category/ijtt/

Research Article

Numerical Investigation of Natural Convection Heat Transfer between Two Vertical Plates with Symmetric Heating

Reda I. El-Ghnam[†*]

[†]Mechanical department, Shoubra Faculty of Engineering, Benha University, Egypt

Accepted 10 Feb 2015, Available online 01 March 2015, **Vol.5, No.1 (March 2015)**

Abstract

The present study deals with laminar natural convection flow in a vertical open-ended channel bounded by isothermal walls. A numerical investigation has been performed to estimate the effect of the channel width and wall-to-ambient temperature difference on natural convection heat transfer and induced flow rate. The results have been obtained for Pr of 0.7, b/L of (0.01 to 0.30) and Ra_b^* of (10^1 to 10^8). Different correlations are deduced to relate each of Nusselt number, flow velocity, flow temperature, thermal entrance length and Reynolds number with modified Rayleigh number and the width-to-length ratio of the channel. Temperature and velocity distribution are potted at different heights along the channel.

Keywords: *Laminar natural convection; two vertical parallel plates; isothermal walls*

1. Introduction

In some applications, natural convection occurs from two closely-spaced vertical plates open at the top and bottom. As one (or both) of the two plates is maintained at a temperature different from the ambient, buoyancy forces induce a vertical flow. Heated fluid rises and exits at the top of the channel, while cool fluid is drawn into the bottom. Depending on the wall temperature, the flow can be laminar or turbulent. Natural convection in vertical channels formed by parallel plates is encountered in many applications ranging from the cooling of electronic equipment to the heating of buildings via Trombe walls. Natural convection heat transfer has been a reliable, cost-effective cooling method for the fast growing electronic industry where hundreds of thermal connection modules are accommodated on a small base. The heat released should be transferred from the surface not only to protect them but also for longer life. An array of rectangular fins used in heat sinks may be idealized by this geometry. Also is encountered in domestic convectors, and dry cooling towers. Also this geometry is considered to simulate the cooling process through the channel formed by plate type fuel elements in the core of plate type reactors.

Elenbaas carried out a detailed study of the thermal characteristics of cooling by natural convection in smooth parallel-walled vertical channels. This pioneering experimental work laid the foundation for the study of natural convection in vertical channels of isothermal parallel plates. More investigations have since followed, especially for the case in which both walls of the channel are heated above ambient. Bodoia *et al*. presented the first numerical simulation on natural convection in a 2D isothermal vertical channel.

The results were compared with those in Ref. (W. Elenbaas, 1942) and showed quite good agreement except for low Rayleigh numbers. Moreover, they characterized two asymptotic regimes for laminar convective flows in vertical channels: fully developed laminar free convection at low Rayleigh numbers and free convective flow along a vertical flat plate for high Rayleigh numbers. Sparrow, *et al*. obtained some numerical results for the heat transfer in a vertical channel using fluids with Prandtl numbers ranging from 0.7 to 10.0. The results showed that increasing the Prandtl number enhances the heat transfer rate through the channel.

Naito and Nagano have investigated the effect of buoyancy on the hydrodynamic and thermal characteristics of downward-flow laminar convection in the entrance region between inclined parallel plates. Numerical solutions are given for three thermal conditions of parallel plates with uniform wall temperature or insulation. The values of local Nusselt number became smaller than those of a horizontal channel with increasing the inclination angles. Naylor *et al*. have performed a numerical study for steady two-dimensional laminar free convection between isothermal vertical plates. The full elliptic form of the Navier-Stokes and energy equations were solved using

*Corresponding author: **Reda I. El-Ghnam,** Tel.: +20 1111150706

novel inlet flow boundary conditions. The solutions were presented for Pr=0.7, $50 \leq Gr_b \leq 5x10^4$ and channel aspect ratio of L/b=10, 17 and 24 respectively. Comparisons with the approximate boundary-layer results show that a full elliptic solution is necessary to get accurate local quantities near the channel entrance. Straatman *et al*. have carried out a numerical and experimental investigation of free convection from vertical isothermal, parallel-walled channels with adiabatic extensions of various sizes and shapes. The experiments were performed with ambient air using a Mach-Zehnder interferometer. In all cases, the adiabatic extensions showed an increase in heat transfer. The increase varied from 2.5 at low Rayleigh number to 1.5 at high Rayleigh number. Lee investigated numerically the effects of unheated entry or unheated exit sections on natural convection in vertical channels with isothermal or iso-flux walls. The results were obtained by means of the boundary layer approximation. An important finding was appeared that an unheated exit determines larger heat transfer and flow rate than an unheated entry does.

Straatman *et al*. have studied the effect of inclination of an isothermal, parallel-walled channel with respect to gravity. The results obtained show that the overall heat transfer from the channel is reduced as the inclination angle increased, and also the overall channel flow rate decrease with increase of the inclination angle. Floryan and Novak have investigated numerically the free convection heat transfer in multiple parallel vertical channels with isothermal walls. Different systems consisting of two, three and an infinite number of channels located side by side and with aspect ratios ranging from 5 to 20 and for Grashof numbers up to 10^5 were considered. The results show that the heat transfer in a channel is affected by its interaction with the neighbouring channels. Roberts and Floryan have investigated numerically the convective cooling of assemblies of electronic circuit boards. The inlet-rounded corners were done to inhibit separation and to explore the resulting improvements in both local and global cooling effectiveness. The fluid is at ambient temperature and its motion toward the channel inlet is described by the Jeffrey-Hamel solution.

Campo *et al*. presented numerical solutions to the wall temperature distribution and the thermal and fluid-dynamic fields in a channel with partially iso-flux heated parallel plates. It was found that a reduction in the maximum wall temperature was observed when an insulated extension was placed downstream of the heated part; the larger the Rayleigh numbers the less relevant the reduction. Shahin and Floryan analyzed numerically the chimney effect in a system of isothermal multiple vertical channels. Each channel had an adiabatic extension. It was observed that the interaction between multiple vertical channels increases the induced flow rate and that the associated chimney effect is stronger than in a single channel with adiabatic extensions. Wirtz and Haag have obtained experimental results for isothermal symmetrical heated plates with an unheated entry channel portion. It was found that the flow was quite insensitive to the presence of the unheated entry section for large channel spacing, while it was severely affected when the gap spacing is small.

Azevedo and Sparrow have performed experiments on an inclined, isothermal channel using water as the convecting fluid. Three modes of heating were investigated; heating both walls, top wall only heated, and bottom wall only heated. Correlations describing this modification were obtained. Miyamoto *et al*. have determined experimentally the heat transfer coefficient in case of turbulent natural convection flow in an asymmetrically heated vertical channel where two vertical parallel plates formed the channel. One plate was heated by imposing a uniform heat flux along the plate and the opposite plate was adiabatic. The channel was open at the bottom and top. Experiments were performed using channel widths of 50, 100 and 200 mm.

Sparrow and Ruiz have obtained useful heat transfer data for natural convection in divergent vertical channels to visualize the flow in the channels, and to develop a universal Nusselt number correlation for divergent, convergent, and parallel-walled channels. The experiments are performed with water as a working fluid (Pr=5). The measured Nusselt numbers for the divergent channel are brought into tight correlation with those for the convergent and parallel walled channels by using correlating parameters based on the maximum inter wall spacing as the characteristic dimension. Krishnan *et al* have investigated experimentally natural convection and surface radiation between three parallel vertical plates, symmetrically spaced, with air as the intervening medium. The analysis consists of heating the central plate at different levels and recording the temperatures of both the central and the side plates at steady state conditions. The measurements were performed for a range of emissivity $0.05 \leq \mathbf{e} \leq 0.85$, aspect ratio $2.38 \leq A \leq 17$, and total heat flux $32 \leq q \leq 1590$ W/m2. Numerical investigation on the transport mechanism of laminar natural convection motion of a Trombe-wall channel and turbulent combined convection between two vertical parallel plates that were uniformly healed were performed by Inagaki and Komori. The results showed significant deviation between the obtained Nusselt number and previous predictions for the case of semi-infinite plates due to the effects of vertical thermal diffusion and free space stratification.

The heat transfer characteristics of natural convection flow in a rectangular cross-sectional vertical finned channel were experimentally investigated by Daloglu and Ayhan. The results show that the Nusselt number for finned channels is less than that for smooth channels for values of modified Rayleigh number ranging from 20 to 90 and length-to-width of 66. Habib *et al*. presented the results of velocity measurements of natural convection in

symmetrically and asymmetrically heated vertical channels. In the first case of symmetrical flow, the two channel plates were both kept at a constant temperature higher than the ambient. In the second case of asymmetrical flow, one plate was kept at a temperature higher than the ambient temperature while the other plate was kept at a temperature lower than the ambient temperature. The velocity measurements were performed using a Laser Doppler Anemometer. Anwar investigated the problem of buoyancy driven turbulent natural convection flow in a vertical channel numerically. The investigation is limited to vertical channels of uniform cross-section (parallel-plate channels) but with different modes of heating. Singh and Paul had studied the transient free convective flow of a viscous incompressible fluid between two parallel vertical walls when convection between the vertical parallel walls is set up by a change in the temperature of the walls as compared to the fluid temperature. A non-dimensional parameter is used in order to characterize the vertical wall temperature with respect to the fluid temperature. Tanda investigated the effect of repeated horizontal protrusions on the free convection heat transfer in a vertical, asymmetrically heated, channel experimentally. The protrusions have a square section and are made of a low thermal-conductivity material.

Experiments were conducted by varying the number of the protrusions over the heated surface (whose height was held fixed) and the aspect ratio of the channel. The convective fluid was air and the wall-to-ambient air temperature difference was set equal to 45 K. Ospir *et al*. represented an experimental and numerical study of the flow in an asymmetrically heated vertical plane channel. The experiments are carried out in water for modified Rayleigh numbers in a range corresponding to the boundary layer flow regime. Mokni expressed a numerical investigation of mixed convection in a vertical heated channel. This flow results from the mixing of the up-going fluid along walls of the channel with the one issued from a flat nozzle located in its entry section. The fluid dynamic and heat-transfer characteristics of vented vertical channels were investigated for constant heat-flux boundary conditions.

Cakar studied the steady-state natural convection from vertically placed rectangular fins numerically by means of a commercial CFD program called ICEPAK. The effects of geometric parameters of fin arrays on the performance of heat dissipation from fin arrays are examined. A combined convection process between two parallel vertical infinite walls, containing an incompressible viscous fluid layer and a fluid saturated porous layer had been presented analytically by Srivastava and Singh. Qing *et al*. presented the experimental research on the steady laminar natural convection heat transfer of air in three vertical thin rectangular channels with different gap clearance. The much higher ratio of width to gap clearance (60–24) and the ratio of length to gap clearance (800–320) make the rectangular channels similar with the coolant flow passage in plate type fuel reactors.

Numerical simulations are performed to study the transition of the development of the thermal boundary layer of air along an isothermal heated plate in a large channel which is bounded by an adiabatic plate by Ali S. *et al*. The channel width was varied from 0.04 m to 0.45 m and the numerical results of the maximum values of the flow velocity, turbulent kinetic energy were recorded along the vertical axis to examine the critical distance of the developing flow. An experimental investigation of natural convection heat transfer in heated vertical ducts dissipating heat from the internal surface is presented by Roul and Ramesh. The ducts are open-ended and circular in cross section. Heat transfer experiment was carried out for four different channels of 45 mm. internal diameter and 3.8 mm thickness with length varying from 450 mm to 850 mm. Ratios of length to diameter of the channel are taken as L/D = 10, 12.22, 15.56, and 18.89. Wall heat fluxes are maintained at q"=250 to 3341 W/m^2. A systematic experimental database for the local steady state natural convection heat transfer behaviour is obtained. The effects of L/D ratio and wall heating condition on local steady-state heat transfer phenomena are studied.

From the review of the pertinent literature presented above, it can be inferred that natural convection in the vertical channel geometry has received considerable attention. In spite of this, there exists scope for further investigation of heat transfer and fluid flow characteristics for this kind of geometries. The present paper performs a numerical study to investigate the characteristics of both heat transfer and induced flow of natural convection in an open-ended vertical channel, bounded by isothermally heated walls. Heat transfer characteristics include the temperature distribution at different heights and progress of average temperature along the channel. In addition, thermal boundary layer characteristics are investigated including thickness and entrance length. Beside, the present work addresses the flow characteristics involving average velocity through the channel, natural Reynolds number and velocity distribution along the channel. The range of study extends from the fully-developed channel flow regime to the boundary-layer regime for the single vertical plate. Different correlations are deduced in the present work to relate each of flow velocity, flow temperature, thermal entrance length and Reynolds number with modified Rayleigh number. In the present study the heat transfer parameters (Nusselt and Rayleigh numbers) are based on the channel width to highlight the role of the channel width.

2. Numerical Details

2.1 Governing Equations

The governing equations of laminar, steady and two-dimensional natural convection with Boussinesq approximation inside the channel are:

$$\frac{\partial u}{\partial x}+\frac{\partial v}{\partial y}=0 \quad (1)$$

$$u\frac{\partial u}{\partial x}+v\frac{\partial u}{\partial y}=-\frac{1}{\rho}\frac{\partial p}{\partial x}+\nu\left(\frac{\partial^2 u}{\partial x^2}+\frac{\partial^2 u}{\partial y^2}\right) \quad (2)$$

$$u\frac{\partial v}{\partial x}+v\frac{\partial v}{\partial y}=-\frac{1}{\rho}\frac{\partial p}{\partial y}+\nu\left(\frac{\partial^2 v}{\partial x^2}+\frac{\partial^2 v}{\partial y^2}\right)+g\beta\left(T-T_\infty\right) \quad (3)$$

$$u\frac{\partial T}{\partial x}+v\frac{\partial T}{\partial y}=\alpha\left(\frac{\partial^2 T}{\partial x^2}+\frac{\partial^2 T}{\partial y^2}\right) \quad (4)$$

Introducing the following dimensionless variables

$$x^*=\frac{x}{b},\ y^*=\frac{y}{b},$$
$$v^*=\frac{v}{\alpha/b},\ u^*=\frac{u}{\alpha/b},$$
$$\theta=\frac{T-T_\infty}{T_s-T_\infty}\ and\ p^*=\frac{p}{\rho\alpha^2/b^2}$$

Equations 1-4 become

$$\frac{\partial u^*}{\partial x^*}+\frac{\partial v^*}{\partial y^*}=0$$

$$u^*\frac{\partial u^*}{\partial x^*}+v^*\frac{\partial u^*}{\partial y^*}=-\frac{\partial p^*}{\partial x^*}+\Pr\left(\frac{\partial^2 u^*}{\partial x^{*2}}+\frac{\partial^2 u^*}{\partial y^{*2}}\right)$$

$$u^*\frac{\partial v^*}{\partial x^*}+v^*\frac{\partial v^*}{\partial y^*}=-\frac{\partial p^*}{\partial y^*}+\Pr\left(\frac{\partial^2 v^*}{\partial x^{*2}}+\frac{\partial^2 v^*}{\partial y^{*2}}\right)+\Pr\ Ra_b\Theta$$

$$u^*\frac{\partial \Theta}{\partial x'}+v^*\frac{\partial \Theta}{\partial y^*}=\left(\frac{\partial^2 \Theta}{\partial x^{*2}}+\frac{\partial^2 \Theta}{\partial y^{*2}}\right)$$

Where

$$Ra_b=\frac{g\beta(T_s-T_\infty)b^3}{\upsilon\alpha}\quad and\ \Pr=\frac{\upsilon}{\alpha}$$

2.2 boundary conditions

The system of Eqs. (1, 2, 3 and 4) will be solved in the entire domain and a set of boundary conditions prescribed along the channel boundary is required.

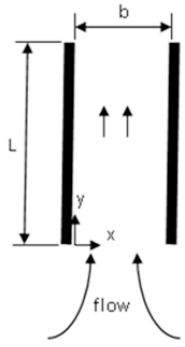

Figure 1: Coordinate system

It will be assumed in the present discussion that the walls are heated and that the flow is consequently upward through the channel. The coordinate system shown in Fig. 1 will be used in the analysis where b and L are width and height of the channel respectively.

2.2.1 Left and right walls

In the present analysis it will be assumed that both walls of the channel are heated to the same uniform temperature.

$$At\ x=0\ and\ x=b: u\ =\ 0, v\ =\ 0, T\ =\ T_w$$

2.2.2 Channel inlet

When the boundary conditions are expressed in pressure at the inlet, the generalized Bernoulli theorem is used to take into account the pressure loss between the upstream and the entry of the channel (upstream velocity assumed to be zero and the pressure is equal to p_∞).

$$p_\infty+0=p_{in}+\frac{\rho v_{in}^2}{2}$$

i.e.:

$$p_{in}-p_\infty=-\frac{\rho v_{in}^2}{2}$$

The pressure therefore falls across the inlet section from p_∞ to $p_\infty-\frac{\rho v_{in}^2}{2}$, i.e., the pressure on the inlet plane is below ambient.

Then the inlet boundary condition can be written as:

$$At\ y=0:\ inlet\ gauge\ total\ pressure=p_{in}-p_\infty+\frac{\rho v_{in}^2}{2}=0$$

It is also assumed that there is no heat transfer to the fluid in the inlet section so that on the inlet plane the fluid is at the ambient temperature, i.e.:

$$At\ y=0:\ T\ =\ T_\infty$$

When boundary conditions are written on velocity, the flow is defined to be normal to the boundary, i.e.:

$$At\ y=0:\ \frac{\partial v}{\partial y}=u=0$$

2.2.3 Channel outlet

Because the flow leaving the channel is essentially parallel to the walls of the channel, the pressure on the exit plane is essentially uniform and equal to the ambient pressure, p_∞. Then the outlet boundary condition can be written as:

$$at\ y=L: outlet\ gauge\ pressure=p_{out}-p_\infty=0$$

When boundary conditions are written on velocity, the flow is defined to be normal to the boundary, i.e.:

$$At\ y=L:\ \frac{dT}{dy}=\frac{\partial v}{\partial y}=u=0$$

2.3 Examination of Grid Resolution

A steady-state two-dimensional solution for the problem was obtained using commercial finite volume code (Fluent 6.2). Fluent 6.2 CFD package was used to create a simple two dimensional model for the channel shown in figure (1). Uniform structural grids were used. The ability of FLUENT code to accurately reproduce published results is validated by many researchers before. In the present study the dependence examinations of the numerical results on different grid resolution parameters are performed.

a) Distribution of the Grid Density

The present and all of the previous examinations concluded that for the considered problem, the highest gradient is in the boundary layer around the walls and gradually reduces as we go far from the wall. So non-uniform grid is used for the solution domain with the grid near the surface of the wall is sufficiently fine to resolve the boundary layer near the wall.

b) Normal Distance, Δn

The effect of normal distance, Δn, between wall surface and the first nodes near the wall, fig. 2, on the numerical results is examined. The importance of this distance is that it used for calculating the local Nusselt numbers and in turn average Nusselt number which represent the amount of heat released from the wall for different temperature difference between the wall surface and ambient temperature.

At wall surface

$$h(dA)(T_w - T_\infty) = -k(dA)\frac{\partial T}{\partial n}\Big|_{x=0}$$

Where n is the normal direction

Rearranging the equation yields

$$\frac{hb}{k} = -\frac{\partial \Theta}{\partial N}\Big|_{x=0}$$

Where $\theta = \frac{T-T_\infty}{T_w-T_\infty}$ and $N = n/b$

Then

$$Nu_b = -\frac{\partial \Theta}{\partial N}\Big|_{x=0}$$

in the present study local Nusselt number is calculated numerically as:

$$Nu_b = -\frac{\partial \Theta}{\partial N}\Big|_{x=0} = \frac{\theta_1 - \theta_2}{\Delta N}$$

Where $\Delta N = \Delta n/b$

It is evidenced by above equation that the accuracy of local Nusselt number depends on the value of $\Delta n/b$.

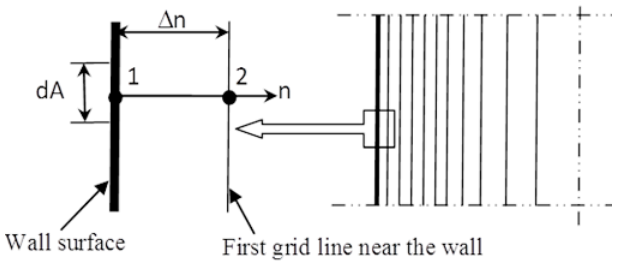

Figure 2: Schematic diagram of numerical system

c) Number of Points on the Wall Surface

The average Nusselt number is calculated using numerical integration as:

$$\overline{Nu} = \frac{1}{L}\int_0^L Nu_b\, dy$$

So the accuracy of the numerical integration depends on the number of points on the wall surface.

It is clear from the above analysis that the numerical results of average Nusselt number depends on the following grid resolution parameters.

1) Distribution of grid density near the wall.

2) The normal distance between the wall surface and first nodes, Δn

3) Number of points on the wall surface.

Different values of the above parameters are tested and the percentage differences in the average number, $\overline{Nu}$, are found to be less than 5% for different values of the Ra_b^*. The grid resolution of 20000 quadrilateral cells and 100 points on the wall surface and having a relative normal distance Δn/b of 0.005 is used in all the calculations in the present work.

The system here consists of two vertical walls having length L which is maintained at a constant temperature of T_w and with channel width b, figure (2). A two-dimensional model representative of channel geometry has been developed. The computational grid for the problem under consideration is generated by using a commercial grid generator GAMBIT and the numerical calculations are performed in the full computational domain using FLUENT for varying conditions of modified Rayleigh number Ra_b^*. The second order upwind scheme is used to discretize both of momentum and energy equations. The semi implicit method for the pressure linked equations (SIMPLE) has been used to pressure-velocity coupling. A convergence criterion of 10^{-3} is used for continuity, while 10^{-6} is used for the x- and y-components of momentum equation and 10^{-8} is used for energy equation.

3. Results and Discussion

3.1 Average wall heat transfer ($\overline{Nu}_b$)

First, the average Nusselt number $\overline{Nu}_b$ was plotted against the Rayleigh number Ra_b, both of which are based on the channel width b, to highlight the effect of the channel width, Fig. 3, where $\overline{Nu}_b$ and Ra_b represent the dimensionless heat transfer rate and the dimensionless plate-to-ambient temperature difference respectively. It is clear from the figure that the width-to-length ratio b/L has an influence on the heat transfer characteristics of vertical channels.

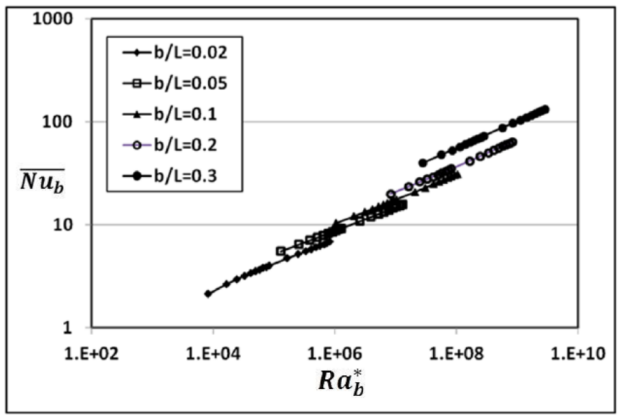

Figure 3: Variation of average Nusselt number $\overline{Nu}_b$ with both of aspect ratio b/L and Rayleigh number Ra_b

To obscure the role of the channel width b, the traditional form for presenting heat transfer results for natural convection in channels is adopted here. In which the modified Rayleigh Ra_b^* ($Ra_b^* = b/L \times Ra_b$) is utilized instead of Ra_b. This presentation yields excellent correlation of the data as demonstrated by fig. 4.

It can be seen that the power-law expression provides an excellent representation of all the numerical data of Fig. 4 as:

$$\overline{Nu}_b = 0.65(Ra_b^*)^{0.242}$$

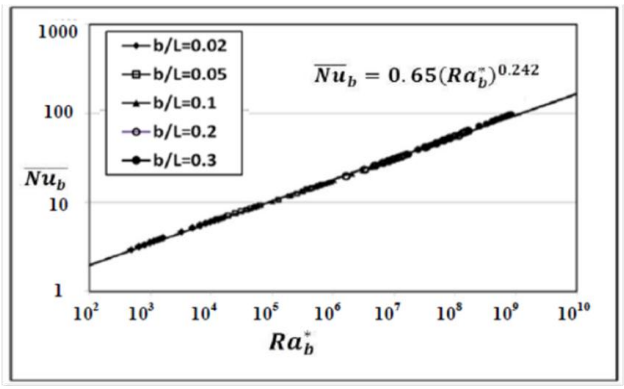

Figure 4: Variation of average Nusselt number $\overline{Nu}_b$ with modified Rayleigh number Ra_b^*

3.2 Local Wall Heat Transfer (Nu_b)

Fig. 5 shows the local Nusselt number nu_b for all studied values of both of wall-to-ambient temperature difference and channel width. The figure illustrates the dependence of local Nusselt number nu_b on both of modified Rayleigh number R_b^* and dimensionless height y/L. The relation between nu_b, Ra_b^* and dimensionless height y/L can be correlated as:

$$Nu_b = 0.4087(Ra_b^*)^{0.24}(y/L)^{-0.385}$$

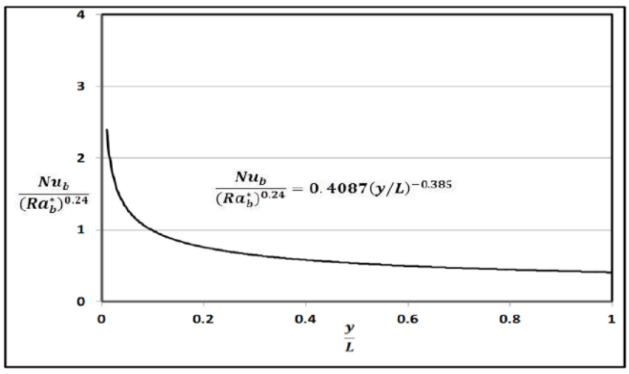

Figure 5: Variation of local Nusselt number Nu_b with both Rayleigh Ra_b^* and dimensionless height y/L

The figure shows that the maximum value of the local Nusselt number occurs at the channel inlet; whereas the least value occurs at the channel exit. This is due to that the fluid temperature increases as fluid rises through the channel. So, the temperature difference between the wall and fluid decreases and in turn the local heat transfer rate decreases.

3.3 Average Temperature along the Channel ($\bar{\theta}$)

Figure 6 shows the sectional average dimensionless temperature $\bar{\theta}$ for all studied values of both of wall-to-ambient temperature difference and channel width. The figure shows the dependence of the sectional average dimensionless temperature $\bar{\theta}$ on both of modified Rayleigh number R_b^* and dimensionless height y/L. The relation between $\bar{\theta}$ and both of Ra_b^* and y/L can be correlated as:

$$\bar{\theta} = 2.8338(Ra_b^*)^{-0.234}(y/L)^{0.3869}$$

The figure shows that the value of the sectional average dimensionless temperature $\bar{\theta}$ (bulk temperature of the fluid) increases steadily along the flow direction. This is due to that the channel wall is constantly heated and the heat flux from the wall to the fluid via convection is constantly added. The figure shows that the maximum value of the sectional average dimensionless temperature $\bar{\theta}$ occurs at the channel exit; whereas the least value occurs at the channel inlet.

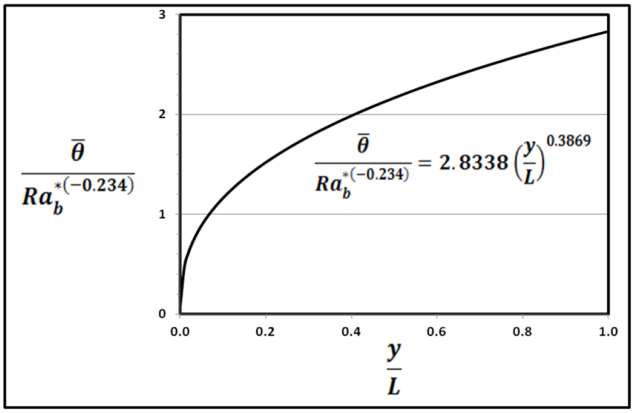

Figure 6: Variation of sectional average dimensionless temperature θ with both of Rayleigh Ra_b^* and dimensionless y/L

3.4 Thermal Boundary Layer

In the present study the thickness of the thermal boundary layer δ_t at any location along the wall is defined as the distance from the wall at which the temperature difference $T_w - T = 0.99(T_w - T_\infty)$ as shown in figure 7.

Rearrange

$$T - T_\infty = 0.01(T_w - T_\infty)$$

$$\frac{T - T_\infty}{T_w - T_\infty} = 0.01$$

$$\theta_{\sigma_t} = 0.01$$

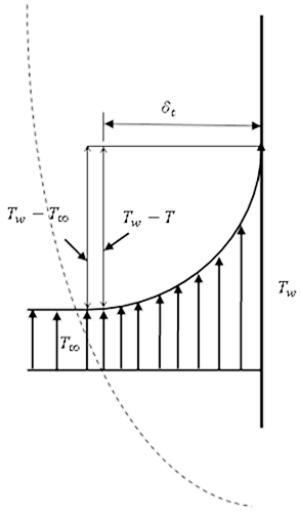

Figure 7: Definition of thermal boundary layer thickness

Thermal boundary layers are plotted for different values of modified Rayleigh number. The figure shows that the boundary layers formed on each wall of the channel increase in thickness with vertical height y/L. It is shown from the figure that the two limiting types of flow can exist. If R_b^* is small enough, the boundary layers eventually join at the center as in internal forced convection and the flow at the exit is fully developed. I.e. in this case, a type of fully developed flow would be expected to exist. If the R_b^* is large enough, the boundary layers are still developing at the exit and the flow will essentially consists of boundary layers on each wall with a uniform flow at temperature T_∞ between the boundary layers. Under these circumstances the plates behave like isolated vertical plates in an infinite fluid and it is to be expected that a boundary-type relation for the heat transfer rate will apply. Figure 8 shows that the development of the boundary layers is influenced by R_b^*.

It is clear from the figure that the most real flows are not well described by either of these two limiting solutions. For this reason, a numerical solution of the governing equations must usually be obtained. The figure shows that the Elenbaas fully developed regime is shown to exist only as a very special limiting case of lower R_b^*. There is wide acceptance that the Elenbaas fully developed regime exists at low Rayleigh numbers, in which the Nusselt number becomes directly proportional to the Rayleigh number. It is clear from figures 4 and 8 that the spacing of the plates determines the size of the heat transfer coefficient. If plates are so far apart (higher R_b^*) that the boundary layers do not interfere and heat transfer is a maximum. As the plates are moved closer together, (lower R_b^*), the boundary layers interact and the rate of heat transfer decreases. In closely-spaced plates, viscous forces result in lower flow velocity which limits heat transfer.

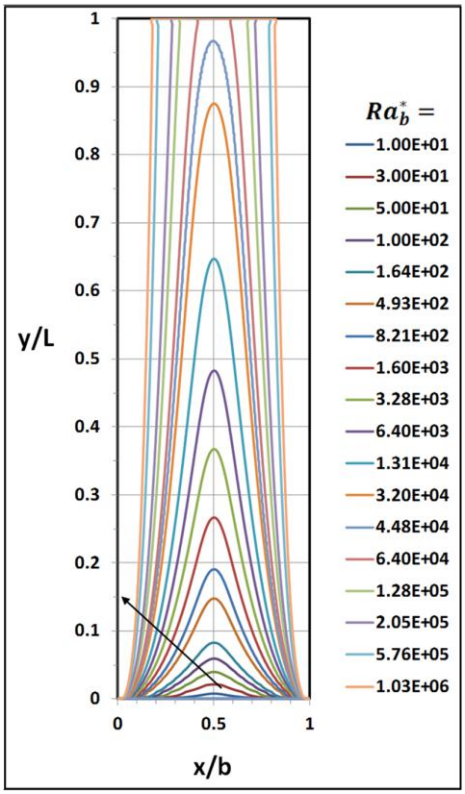

Figure 8: Thermal boundary layer thickness for different values of modified Rayleigh number Ra_b

3.5 Thermal Entrance Length L_{e_t}

As shown in fig. 8, the fully developed condition is often met at some distance away from inlet which is called the entrance region length. Fig. 8 shows that if Ra_b^* is low enough, it may well be that the entrance region length is ignorable small so that flow in the entire length of the channel can be considered fully developed. The figure shows also that if Ra_b^* is high enough the fully developed flow is never realized. The distance downstream from the inlet to where the flow becomes fully developed flow is called the thermal entrance length L_{e_t}. The relative thermal entrance length $\frac{L_{e_t}}{L}$ required for fully developed flow is obtained by a complete solution of the flow and thermal field in the entire region. Figure 9 shows that the relative thermal entrance length $\frac{L_{e_t}}{L}$ increases with the increase of modified Rayleigh number Ra_b^*. The following correlation relates the value of the relative thermal entrance length $\frac{L_{e_t}}{L}$ and modified Rayleigh number Ra_b^* as:

$$\frac{L_{e_t}}{L} = 0.0068\left(Log\ (Ra_b^*)\right)^{3.1794}$$

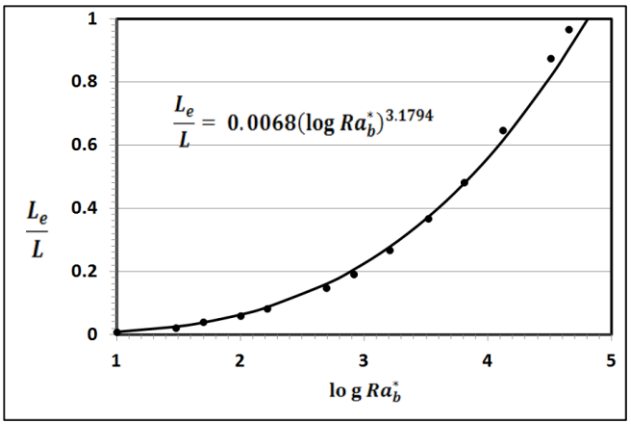

Figure 9: variation of the relative thermal entrance length $\frac{L_{e_t}}{L}$ with modified Rayleigh number Ra_b^*

3.6 Temperature Distribution along the Channel

The temperature distribution along the channel helps to explain the heat transfer behaviour from the fully developed limit to the isolated plate limit. The influences of both of modified Rayleigh number R_b^* and dimensionless height y/L on the distribution of dimensionless temperature θ along the channel are presented in figure 10. It is shown from fig. 10 that the axial dimensionless temperature profiles which are plotted at different heights show a general trend i.e. the temperature besides the isothermal walls is maximum which then drops to the channel center. The profiles also show a gradual increase in the fluid temperature from the inlet towards the downstream of the channel in all the cases due to the increase of the temperature gradient at the wall along the channel. The temperature profile continues to change with y due to continuous heating, and the only situation in which the flow temperature is invariant with y is when the heating is complete, i.e. the fluid is in thermal equilibrium with the channel wall.

It is shown from figure 10.a, $R_b^* = 41$, that the temperatures at section y/L=0.05 is greater than the inlet temperature ($\theta = 0$). So the relative thermal entrance length $\frac{L_{e_t}}{L}$ is less than 0.05 which means that at low Rayleigh number a fully developed heat flow in a channel can be considered. The figure also illustrates that at low Rayleigh number, the channel exit temperature is nearly equals the wall temperature and temperature distribution at sections y/L=0.8 and y/L=0.9 are nearly coincide with the temperature distribution at the channel exit. It is expected from the figure that for $R_b^* < 41$ the sections at which the temperature profile is invariant with y and the heating is complete are less than y/L=0.8.

With the increase of R_b^*, figure 10.b, the centerline temperature decreases towards the inlet temperature but still above it. With more increase of R_b^*, figure 10.c, the temperature profile at section y/L=0.2 intersects the x axis ($\theta = 0$) at a line that lies outside the thermal boundary layer. With more and more increase of R_b^*, figures 10.d to 10.h, more temperature profiles intersect the x axis and the line of intersection is wider and thermal boundary layer is thinner until all temperature profiles intersect the x axis and boundary layer heat flow in a channel can be considered.

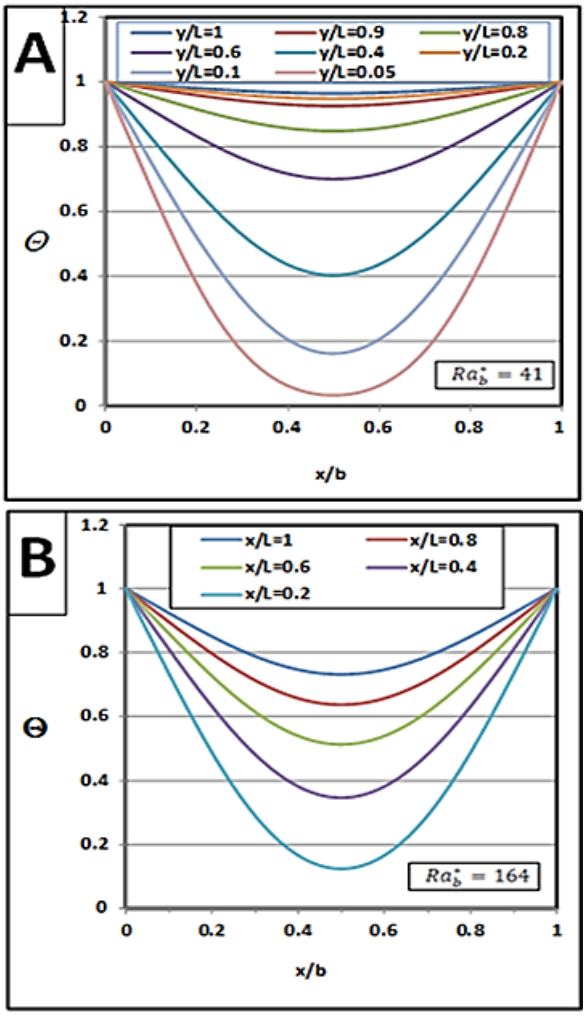

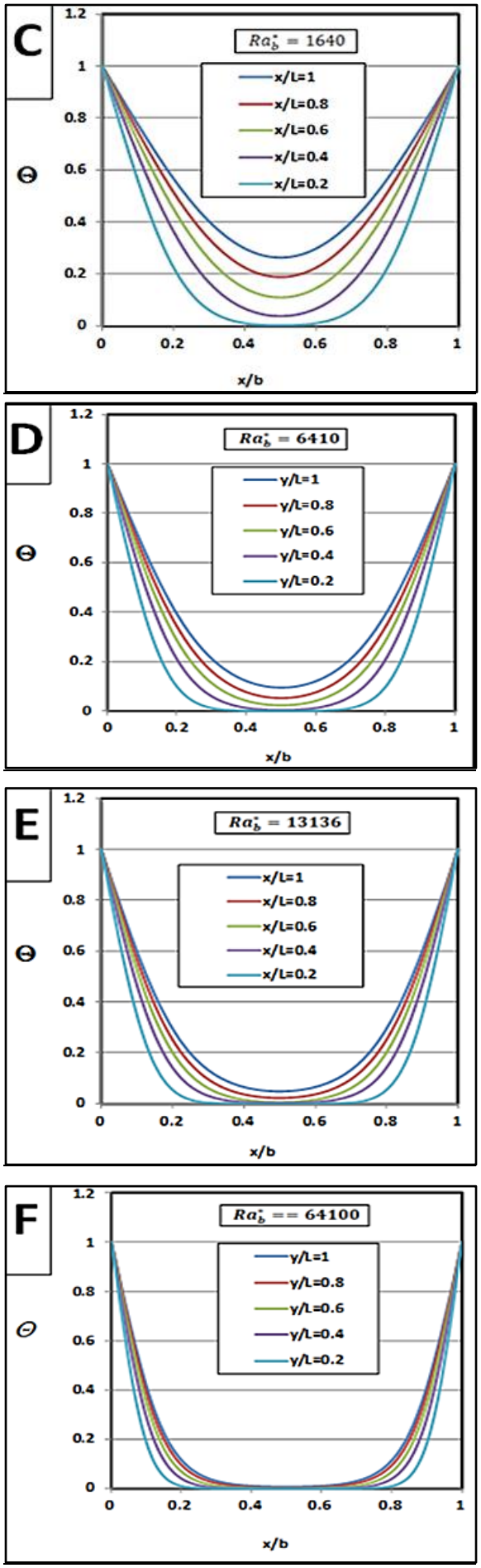

Figure 10: Temperature distribution along the channel at selected dimensionless height y/L

3.7 Average Velocity $\overline{v^*}$and Natural Reynolds Number Re_b

Figure 11 shows the average dimensionless velocity $\overline{v^*}$ for all studied values of both of wall-to-ambient temperature difference and channel width. The figure shows the dependence of the average dimensionless velocity $\overline{v^*}$ on both of modified Rayleigh number R_b^* and width-to-length ratio b/L. The relation between $\overline{v^*}$ and both of Ra_b^* and b/L can be correlated as:

$$\overline{v^*} = 0.52093\ (b/L)^{-1}(\log(Ra_b^*))^{2.986}$$

This indicates that the average velocity increases with the increase of wall-to-ambient temperatures difference and decreases with the increase of the channel width.

Applying the definition of $\overline{v^*}$ gives

$$\overline{v^*} = \frac{\bar{v}b}{\propto} = \frac{\bar{v}b}{\propto}\frac{\nu}{\nu} = \frac{\bar{v}b}{\nu}\frac{\nu}{\propto} = Re_b \times Pr$$

Then the natural Reynolds number can be correlated to the modified Rayleigh number, Prandtl number and the width-to-length ratio of the channel as:

$$Re_b = 0.52093\ (\mathrm{Pr})^{-1}\ (b/L)^{-1}(\log(Ra_b^*))^{2.986}$$

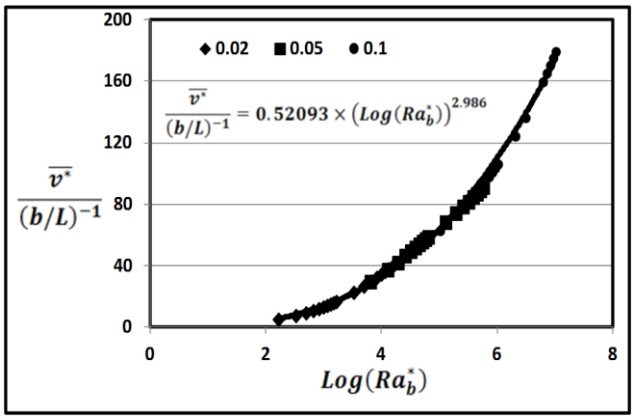

Figure 11: Variation of average dimensionless velocity $\overline{v^*}$ with both of modified Rayleigh Ra_b^* and width-to-length ratio b/L

3.8 Velocity Distribution along the Channel

Figure 12 shows the velocity profiles at the different values of y/L ranging from the channel inlet y/L=0 to channel exit y/L=1.0. Chimney effect can be seen at the channel inlet with fluid rising upwards inside the channel. The velocity profiles along the channel help to explain the flow behavior from the fully developed limit to the isolated plate limit. It is clear from the figure that the velocity profile continues to change with y.

It is shown from figure 12.a, $R_b^* = 164$, that the velocity profiles at all sections are coincident and invariant with y and with one peak at the center, indicating a a fully developed flow in a channel. With the increase of R_b^*, figure 10.b, two velocity peaks appear near to the walls and flow at the channel center is slowed down. With the increase of higher Ra_b^* , the velocity peaks are higher and the velocity at the channel center decreases. In all the cases the peak of the velocity profile appears beside the heated walls as expected; but when R_b^* is increased, the velocity peaks become sharp and move towards the heated walls, indicating a rapid acceleration of the fluid flow near the heated wall.

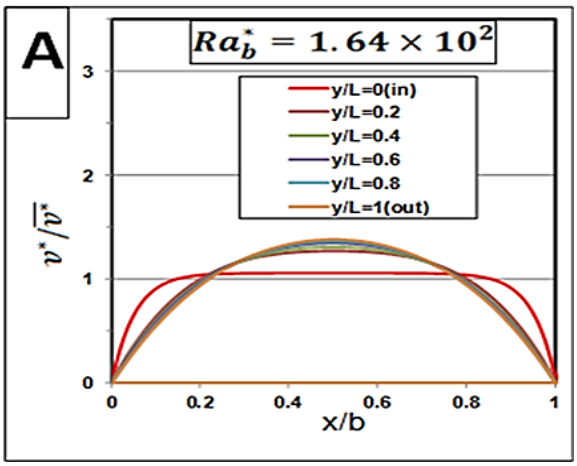

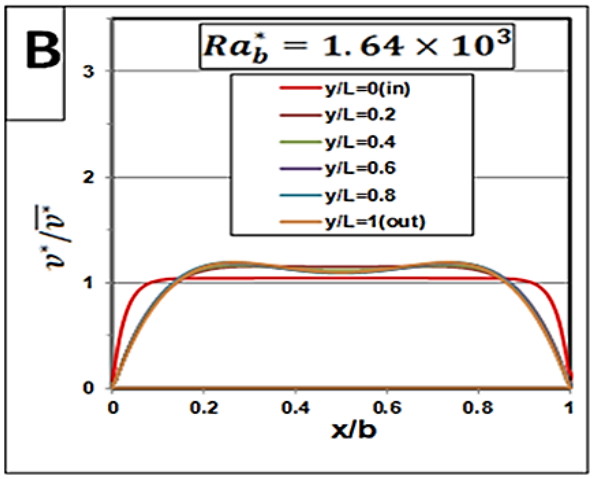

Figures 12.c to 12.f show that for velocity profiles near the channel inlet the magnitude of the velocity drops slowly from their peaks towards the channel center and remain almost flat. For velocity profiles near the channel outlet and particularly at the outlet the magnitude of the velocity drops rapidly towards the channel center. Figures 12.c to 12.f show that for wide range of velocity profiles the magnitude of velocity show a sharp drop towards the channel center and remain almost flat, indicating a situation of the isolated plate limit.

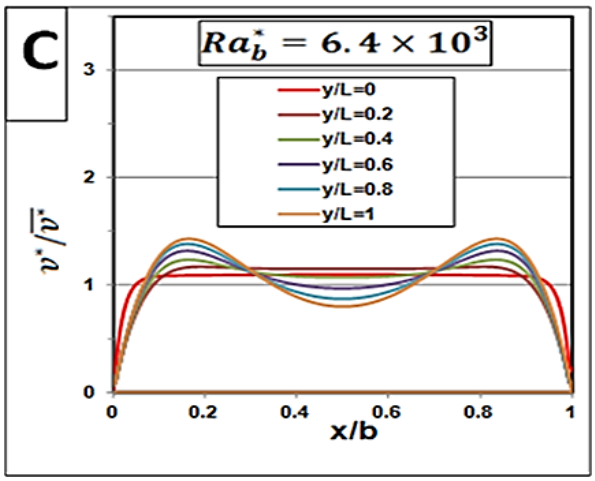

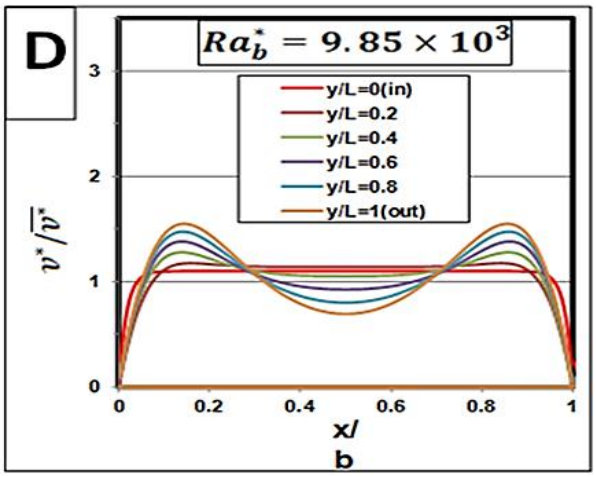

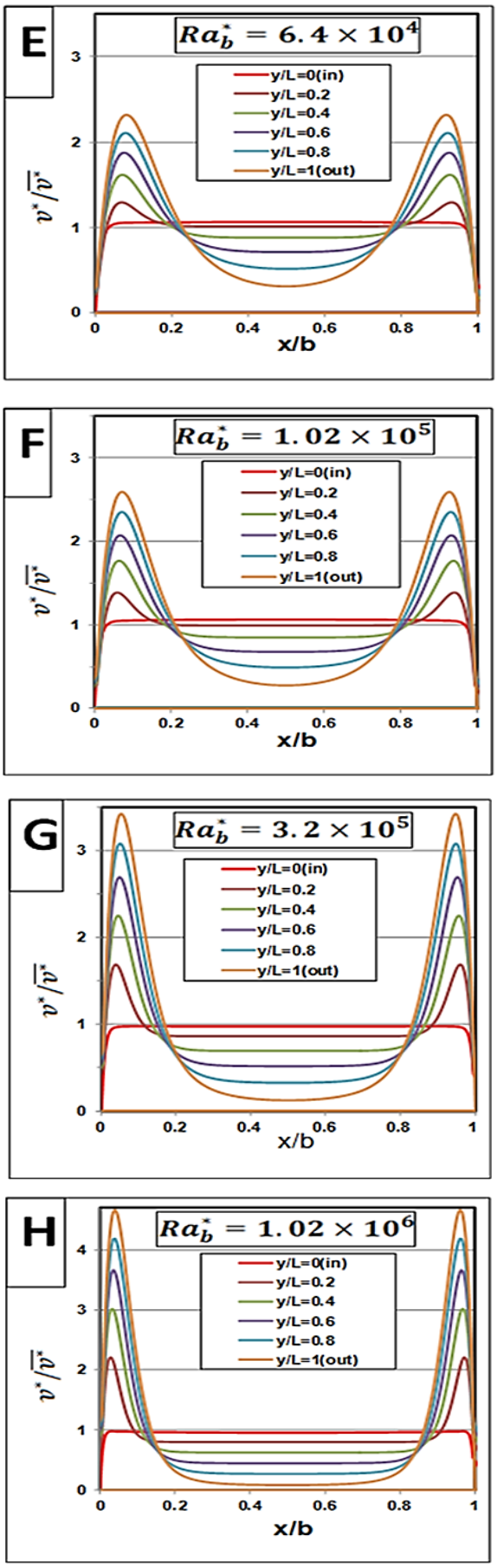

Figure 12: Velocity profiles along the channel at selected dimensionless height /L

It is clear from figure 12.a that the centerline velocities increase along the channel length and are higher than inlet centerline velocity. With the increase of higher Ra_b^*, figure 12.b, the velocity peaks appear and the centerline velocities decrease but still above the inlet centerline velocity. With more increase of Ra_b^*, figure 12.c and 12.d, some of the centerline velocities become below the inlet centerline velocity and for higher Ra_b^*, figures 12.e to 12.h, all of the centerline velocities become below the inlet centerline velocity. This phenomenon is reported in figure 13 for wide range of. Ra_b^*.

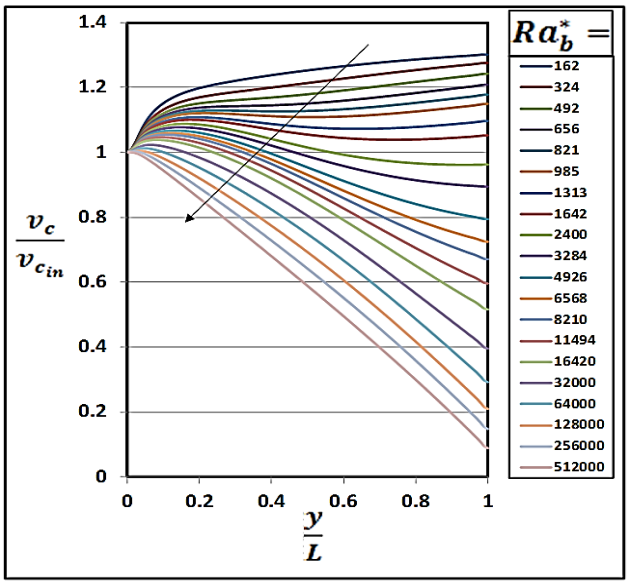

Figure 13: Centre line velocity ration V_c/V_{cin}

4. Comparison with previous published results

For comparison purposes, the present correlation is plotted with correlations developed by previous investigators W. Elenbaas and E. M. Sparrow etc. Fig. 14. The figure shows a remarkable level of agreement.

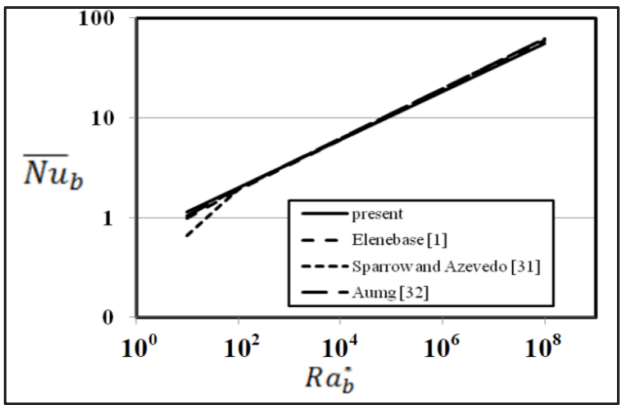

Figure 14: Comparison between the present corrections of average Nusselt number $\overline{Nu}_b$ and corrections developed by previous investigators

Conclusions

Numerical results of the natural convection inside a vertical channel have been presented in this paper giving a particular attention to the effects of the channel width and wall-to-ambient temperature difference combined in one parameter Ra_b^* on the distributions of the velocity and temperature along the channel. This paper presents a parametric variation of the width-to-length ratio b/L and modified Rayleigh number based on the channel width Ra_b^*. Temperature and velocity calculations have been obtained for Prandtl number of 0.7, width-to-length ratio of (0.01 to 0.30) and Rayleigh Ra_b^* of (10^1 to 10^8). Different correlations are deduced in the present work to relate each of Nusselt number, flow velocity, flow temperature, thermal entrance length and Reynolds number with modified Rayleigh number and the width-to-length ratio of the channel. Temperature distribution and velocity distribution are potted at different heights along the channel. The conclusions can be *+*summarized as:

1) To obscure the role of the channel width b, the traditional form for presenting heat transfer results for natural convection in channels is adopted here. In which the modified Rayleigh Ra_b^* ($Ra_b^* = b/L \times Ra_b$) is utilized instead ofRa_b. This presentation yields excellent correlation of the data as: $\overline{Nu}_b = 0.65(Ra_b^*)^{0.242}$
2) The dependence of local Nusselt number nu_b on both of modified Rayleigh number R_b^* and dimensionless height y/L is correlated as: $u_b = 0.4087(Ra_b^*)^{0.24}(y/L)^{-0.385}$.

   The correlation shows that the maximum value of the local Nusselt number occurs at the channel inlet; whereas the least value occurs at the channel exit.
3) The dependence of the sectional average dimensionless temperature $\bar{\theta}$ on both of modified Rayleigh number R_b^* and dimensionless height y/L can be correlated as: $\bar{\theta} = 2.8338(Ra_b^*)^{-0.234}(y/L)^{0.3869}$.

   The correlation shows that the value of the sectional average dimensionless temperature $\bar{\theta}$ (bulk temperature of the fluid) increases along the flow direction and its maximum value occurs at the channel exit; whereas the least value occurs at the channel inlet.
4) It is shown from the numerical results that the two limiting types of flow can exist. If R_b^* is small enough, the boundary layers eventually join at the center as in internal forced convection and the type of fully developed flow would be expected to exist. If the R_b^* is large enough, the boundary layers are still developing at the exit and the flow will essentially consist of boundary layers on each wall with a uniform flow at temperature T_∞ between the boundary layers. Under these circumstances the plates behave like isolated vertical plates in an infinite fluid. It is clear from the figure 8 that the most real flows are not well described by either of these two limiting solutions. For this reason, a numerical solution of the governing equations must usually be obtained.
5) The dependence of the relative thermal entrance length $\frac{L_{e_t}}{L}$ on modified Rayleigh number R_b^* can be correlated as: $\frac{L_{e_t}}{L} = 0.0068\left(Log\ (Ra_b^*)\right)^{3.1794}$

   This indicates that the relative thermal entrance length $\frac{L_{e_t}}{L}$ increases with the increase of modified Rayleigh number Ra_b^*.
6) The dependence of the average dimensionless velocity $\overline{v^*}$ on both of modified Rayleigh number R_b^* and width-to-length ratio b/L can be correlated as: $\overline{v^*} = 0.52093\ (b/L)^{-1}(\log(Ra_b^*))^{2.986}$.

   This indicates that the average velocity increases with the increase of wall-to-ambient temperatures difference and decreases with the increase of the channel width.
7) The results show that while the fluid bulk velocity $\overline{v^*}$ is invariant with respect to y to satisfy the conservation of mass because the channel walls are impervious, in contrast, the fluid bulk temperature $\bar{\theta}$ is not a constant with respect to y. It increases with y due to the heating of the fluid from the channel wall. The temperature of the fluid within a channel, therefore, increases as a function of x and y coordinates. Eventually, when heating in the channel is fully done, the fluid temperature T(x,y) becomes uniform over the entire cross section in equilibrium with the wall temperature.
8) A remarkable level of agreement between the published results and the present numerical predictions was obtained.

Nomenclature

b	channel width (m)
b/L	width-to-length ratio
g	gravitational acceleration (m/s^2)
k	Thermal conductivity (W/m^{o}c)
L	channel length (m)
L_{e_t}	Thermal Entrance Length (m)
Nu_b	local Nusselt number $=\frac{hb}{k} = -\frac{\partial\Theta}{\partial N}\Big\vert_{x=0}$
$\overline{Nu}$	average Nusselt number $=\frac{\bar{h}b}{k} = \frac{1}{L}\int_0^L Nu_b\ dy$
p	pressure (N/m^2)
p_∞	Ambient pressure (N/m^2)
p_{in}	Channel inlet pressure (N/m^2)
p_{out}	Channel outlet pressure (N/m^2)

p^*	Dimensionless pressure = $p/(\rho\alpha^2/b^2)$
Pr	Prandtl number = υ/α
Ra_b	Rayleigh number based on the channel width = $g\beta(T_s - T_\infty)b^3/\upsilon\alpha$
Ra_b^*	modified Rayleigh number based on the channel width= $b/L \times Ra_b$
Re_b	Natural Reynolds Number = $(\bar{v}b)/\nu$
T	temperature (°C)
T_w	Wall temperature (°C)
T_∞	Ambient temperature (°C)
u	velocity components in the x direction (m/s)
u^*	Dimensionless velocity components in the x direction = $u/(\alpha/b)$
v	velocity components in the y direction(m/s)
v_{in}	Channel inlet velocity(m/s)
v^*	Dimensionless velocity components in the y direction = $v/(\alpha/b)$
$\bar{v}^*$	Average dimensionless velocity = $v/(\alpha/b)$
x	Horizontal Cartesian coordinates (m)
x^*	Dimensionless Cartesian coordinate = x/b
y^*	Dimensionless Cartesian coordinate = y/b
y	Vertical Cartesian coordinates (m)
y/L	dimensionless height
Greek symbols	
α	thermal diffusivity (m^2/s)
β	thermal expansion coefficient ($°C^{-1}$)
υ	kinematic viscosity (m^2/s)
ρ	Density (kg/m^3)
θ	Dimensionless temperature = $(T - T_\infty)/(T_s - T_\infty)$
$\bar{\theta}$	sectional average dimensionless temperature = $(T - T_\infty)/(T_s - T_\infty)$
Subscripts	
in	Channel inlet
out	Channel outlet
b	Based on the channel width b
w	Wall
∞	Ambient
superscripts	
*	Dimensionless
-	Average

Author's profile

Reda I. Elghnam is currently Associate Professor of Mechanical Engineering (Power department) at Shoubra Faculty of Engineering, Benha University, Egypt. He has published about 21 papers in referred national and international journals and conference proceedings. His area of research is heat transfer, heat pipes and combustion

References

W. Elenbaas (1942), Heat Dissipation of Parallel Plates by Free Convection, Physica, vol. 9(1), pp. 1–28.

J. R. Bodoia, J. F. Osterle (1962), The Development of Free Convection between Heated Vertical Plates, Trans. ASME, vol. 84 (1), pp 40-43.

E. M. Sparrow, G. M. Chrysler, and L. F. Azevedo (1984), Observed Flow Reversals and Measured Predicted Nusselt Numbers for Natural Convection , ASME Journal of Heat Transfer, Vol.106, pp. 325-330.

E. Naito, and Y. Nagano (1989), The Effect of Buoyancy on Downward and Upward Laminar-Flow Convection In The Entrance Region between Inclined Parallel Plates, International Journal of Heat and Mass Transfer, Vol. 32, No. 5, pp. 811-823.

D. Naylor, J. M. Floryan, and J. D. Tarasuk (1991), A Numerical Study of Developing Free Convection between Isothermal Vertical Plates, ASME Journal of Heat Transfer, Vol.113, No.3, pp. 620-626.

A. G. Straatman, J. D. Tarasuk, and J. M., Floryan (1993), Heat Transfer Enhancement From A Vertical, Isothermal Channel Generated by The Chimney Effect, ASME Journal of Heat Transfer, Vol.115, pp. 395-402.

K. T. Lee (1994), Natural Convection in Vertical Parallel Plates with Unheated Entry or Unheated Exit, Numerical Heat Transfer- Part A 25, pp. 477- 493.

A. G. Straatman, D. Naylor, J. M. Floryan, and J. D., Tarasuk (1994), A Study of Natural Convection between Inclined Isothermal Plates, ASME Journal of Heat Transfer, Vol.116, No.5, pp. 243-245.

J. M. Floryan, and M. Novak (1995), Free Convection Heat Transfer in Multiple Vertical Channels, International Journal of Heat and Fluid Flow, Vol. 16, No. 4, pp. 244-253.

D. A. Roberts, and J. M. Floryan (1998), Heat Transfer Enhancement in the Entrance Zone of a Vertical Channel, ASME Journal of Heat Transfer, Vol. 120, pp. 290-291.

A. Campo, O. Manca, and B. Morrone (1999), Numerical Analysis of Partially Heated Vertical Parallel Plates in Natural Convective Cooling, Numerical Heat Transfer –Part A36, pp. 129-151.

G. A. Shahin, and J. M. Floryan (1999), Heat Transfer Enhancement Generated by Chimney Effect in Systems of Vertical Channels, ASME Journal of Heat Transfer, Vol. 121, pp. 230-232.

R. A. Wirtz, and T. Haag (1985), Effects of Unheated Entry on Natural Convection between Heated Vertical Parallel Plates , ASME Paper, 85- WA/HT-14.

L. F. Azevedo, and E. M. Sparrow (1985), Natural Convection in Open Ended Inclined Channels, International Journal of Heat and Mass Transfer Vol. 107, pp. 893 – 901.

M. Miyamoto, Y. Katoh, J. Kurima, and H. Saki (1986), Turbulent Free Convection Heat Transfer from Vertical Parallel Plates, Heat Transfer, Vol. 4. Hemisphere. Washington, DC, pp. 1593 –1598.

E. M. Sparrow, and R. Ruiz (1988), Experimental Investigation of Parallel Walled and Divergent –Walled open Thermosyphons, International Journal of Heat and Mass Transfer, Vol.31, pp. 1961-1967.

A. S. Krishnan, C. B. Alaji, and , S. P. Venkateshan (2004), Experimental Correlation for Combined Convection and Radiation between Parallel Vertical Plates, Journal of Heat Transfer, Volume 126, Issue 5, pp. 849- 851.

T. Inagaki, K. Komori (1995), Numerical modeling on turbulent transport with combined forced and natural convection between two vertical parallel plates, Int. J. Comput. Meth. A 27, vol. 4, pp. 417–431..

T. Daloglu, Ayhan (1999), Natural Convection in a Periodically Finned Vertical Channel, Int. Commun. Heat Mass Transfer, vol. 26 (8), pp. 1175–1182.

M.A. Habib, S.A.M. Said, S.A. Ahmed, and A. Asghar (2002), Velocity Characteristics of Turbulent Natural Convection in Symmetrically and Asymmetrically Heated Vertical Channels, Experimental Thermal and Fluid Science, vol. 26, pp. 77–87.

S. Anwar (2003), Natural Convection Flow in Parallel-Plate Vertical Channels, M.Sc. Thesis, The King Fahd University of Petroleum and Minerals.

A. K. Singh and T. Paul (2006), Transient Natural Convection between Two Vertical Walls Heated/Cooling Asymmetrically, International Journal of Applied Mechanics and Engineering, Vol.11, No.1, pp.143-154.

G. Tanda (2008), Natural Convective Heat Transfer in Vertical Channels with Low-Thermal Conductivity Ribs, International Journal of Heat and Fluid Flow, vol. 29, pp. 1319–1325.

D. Ospir, C. Chereches, C. Popa, S. Fohanno, and C. Popovici (2009), Flow Dynamics in a Double-Skin Façade, Proceedings of the 3rd WSEAS International Conference on Finite Differences – Finite Elements – Finite Volumes – Boundary Elements.

H. Mokni, G. Mhiri, L. Palec, and P. Bournot (2009), Mixed Convection in a Vertical Heated Channel: Influence of the Aspect Ratio, International Journal of Engineering and Applied Sciences, vol. 5 (1), pp.60-66.

K. M. ÇAKAR (2009), Numerical Investigation of Natural Convection from Vertical Plate Fined Heat Sinks, M.Sc. Thesis, The Middle East Technical University.

N. Srivastava1 and A. K. Singh (2010), Mixed Convection in a Composite System Bounded by Vertical Walls, Journal of Applied Fluid Mechanics, Vol. 3, No. 2, pp. 65-75.

Q. Lu, S. Qiu, G. Su, W. Tian, and Z. Ye (2010), Experimental Research on Heat Transfer of Natural Convection in Vertical Rectangular Channels with Large Aspect Ratio, Experimental Thermal and Fluid Science, vol. 34, pp. 73–80.

A. Alzwayi (2013), M. Paul, Effect of Width and Temperature of a Vertical Parallel Plate Channel on the Transition of the Developing Thermal Boundary Layer, International Journal of Heat and Mass Transfer, vol. 63, pp. 20–30.

M. K. Roul, and R. C. N. Ramesh (2012), Experimental Investigation of Natural Convection Heat Transfer Through Heated Vertical Tubes, International Journal of Engineering Research and Applications (IJERA), Vol. 2, Issue 6, pp.1088-1096.

E. M. Sparrow and L. F. A. Azevedo (1985), Vertical-Channel Natural Convection Spanning between the Fully-Developed Limit and the Single-Plate Boundary-Layer Limit, Int. J. Heat Mass Transfer. Vol. 28, No. 10, pp. 1847-1857

W. Aung (1972), Fully Developed Laminar Free Convection between Vertical Plates, International Journal of Heat and Mass Transfer, vol. 15, pp. 1577-1580.